JOURNAL OF SOLID STATE CHEMISTRY 37, 362–369 (1981)

Lattice Imaging of Extended Defects and Related Phases in Polycrystalline Sr(Ba)$Fe_{18}O_{27}$ (Ferrous W)

F. J. A. DEN BROEDER

Philips Research Laboratories, 5600 MD, Eindhoven, The Netherlands

Received September 15, 1980

The defect structure of polycrystalline $SrFe_{18}O_{27}$ and $BaFe_{18}O_{27}$ (ferrous W) was investigated by TEM using lattice fringe imaging. Various extended defects were identified in the *MS* sequence along the hexagonal *c* direction of the *W* structure (*M* = magnetoplumbite, *S* = spinel). These are isolated (extra) *M* blocks, isolated *S* blocks, and in a few cases isolated S_2 and S_3 blocks, running throughout a whole *W* crystallite along the basal plane. These defects serve to accommodate a local deviation from the stoichiometric *W* composition. In regions of large concentrations of isolated *S* blocks or *M* blocks, they tend to order, forming new compounds M_2S_3, M_4S_5, or M_4S_3. A frequently occurring defect with which no local composition deviation is associated is due to a locally inverse *MS* sequence. It is proposed that this sequential fault originates from a growth accident.

Introduction

In the BaO–*Me*O–Fe_2O_3 system, where *Me* stands for a divalent transition element (Fe, Ni, Co, or Zn) and where BaO may also be replaced by SrO or PbO, several compounds with long-period structures occur. These compounds are called the hexagonal ferrites. The most well-known example is $BaO \cdot 6Fe_2O_3$ with the magnetoplumbite (*M*) structure which is a basis material for the production of permanent magnets. Other compounds are $Ba_2Me_2Fe_{12}O_{22}$ (*Y*), $BaMe_2Fe_{16}O_{27}$ (*W*), $Ba_3Me_2Fe_{24}O_{41}$ (*Z*), $Ba_2Me_2Fe_{28}O_{46}$ (*X*), and $Ba_4Me_2Fe_{36}O_{60}$ (*U*). Although the chemical formulas of these compounds are complex and seem to be unrelated, their crystal structures are closely related. Actually they can be built up from three basic building blocks *S*, *R*, and *T*, by stacking these in certain ways on top of each other along a common *c* axis (*2*). These blocks have a common hexagonal *a* parameter of 5.88 Å but different hexagonal *c* axes (Fig. 1) and consist of hexagonal arrays of oxygen ions. Two oxygen layers can be distinguished, one with four oxygen ions, the other with three oxygen ions and a barium ion. The Me^{II} and the Fe^{III} cations are located in the interstices between the oxygen ions. It is further helpful to distinguish two types of *S* blocks. One has the spinel stoichiometry $Me_2^{II}Fe_4^{III}O_8$, designated by S^0, which has no net charge. The other one is $Fe_6^{III}O_8$ with a net charge of +2, designated by S^{2+}. An *R* block has the formula $(BaFe_6^{III}O_{11})^{2-}$ and is always found in combination with a charged *S* block, forming an $R^{2-}S^{2+}$ unit of $BaO \cdot 6Fe_2O_3$ (*M*). A *T* block has the stoichiometry $Ba_2Fe_8^{III}O_{14}$ and has no net charge; when it is combined with a neutral S^0 block one obtains a TS^0 unit which is the fundamental block of the *Y* phase. Table I shows how the above-mentioned compounds can be symbolized by

0022-9517/81/060362-08$02.00/0

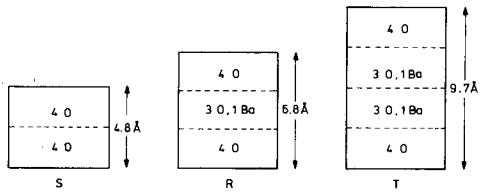

FIG. 1. Schematic construction of fundamental building blocks S, R, and T in the hexagonal ferrites (after (*3*)).

their stacking order and lists the c axes of their constituent blocks. It is to be noted that the complete unit cell of the phases M, W, and Z along the c direction comprises two blocks resulting in a hexagonal structure, whereas the complete unit cell of the phases X, Y, and U along the c direction comprises three blocks resulting in a rhombohedral structure. Apart from those mentioned, other compounds with more complex stacking sequences have been identified (*3–7*). In fact the hexagonal ferrites can be divided into an M_nS series with $n = 1$ (W), $n = 2$ (X); $n = 4$, $n = 6$, and $n = \infty$ (M); and a large M_nY_p series (with n even up to $n = 8$, $p = 27$). In contrast to the members of the M_nS series, those of the M_nY_p series may show polytypism due to permutation of blocks leading to the same chemical formula (*3–7*).

The present paper concerns the compounds ferrous Sr–W and Ba–W, in which the divalent transition metal is Fe^{II}. The S^0 blocks here consist of two molecules of Fe_3O_4. These compounds can be prepared either as single crystals from the melt (*8*) or in polycrystalline form by a solid state reaction between SrO(BaO) and Fe_2O_3 under an appropriate oxygen partial pressure. Whereas crystallization from the melt also gives rise to the formation of other related compounds, it has been shown by X-ray diffraction that the solid state reaction may, depending on firing conditions, lead to the formation of pure W (*9, 10*). It was thought interesting, therefore, to investigate by transmission electron microscopy (TEM) the presence of secondary phases on a microscopic scale and the perfectness of the W crystallites in sintered samples. We made use of lattice fringe imaging by interference of 00.l diffraction spots to reveal stacking sequences along the c direction. The usefulness of this technique in determining stacking sequences in the hexagonal compounds has been demonstrated previously by van Landuyt *et al.* (*11, 12*) and by Hirotsu and Sato (*13*). In this paper we report on the occurrence of some typical defects in W crystallites as well as on the existence of some new compounds in the M–S series that have not been identified so far.

Experimental Procedure

Sample Preparation

Polycrystalline $BaFe_{18}O_{27}$ was obtained from a previous investigation by Lotgering *et al.* (*14*), who described the details of the sample preparation. Polycrystalline $SrFe_{18}O_{27}$ was prepared using similar techniques. After milling the prereacted compact, the powder obtained was either sintered at 1200°C at a reduced oxygen partial pressure, or was hot-pressed at 950°C in pure N_2. The following samples were studied:

Sample I. Sintered $SrFe_{18}O_{27}$. X-Ray diffraction showed predominantly Sr–W with a small amount of Sr–Z.

Sample II. Hot-pressed $SrFe_{18}O_{27}$, which contained Sr–W and some α-Fe_2O_3 accord-

TABLE I

BLOCK CODES AND BLOCK SIZES OF VARIOUS HEXAGONAL FERRITES

Phase	Block code	Total block size (Å)
M	$R^{2-}S^{2+}$	11.6
W	$R^{2-}S^{2+}S^0$ (MS^0)	16.4
X	$R^{2-}S^{2+}R^{2-}S^{2+}S^0$ ($MMS^0 = MW$)	28.0
Y	TS^0	14.5
Z	$R^{2-}S^{2+}TS^0$ (MY)	26.1
U	$R^{2-}S^{2+}R^{2-}S^{2+}TS^0$ ($MMY = MZ$)	37.7

ing to X-ray diffraction and light microscopy.

Sample III. Sintered $BaFe_{18}O_{27}$, containing Ba–W with some Fe_3O_4.

TEM specimens were obtained as 3-mm dia disks, by sawing and polishing to a thickness of 35 μm, followed by ion beam thinning.

Microscopy

The investigation was done with a Philips EM-301 electron microscope (100 kV) with goniometer stage, using a double-tilt specimen holder. To obtain a 00.*l* lattice fringe image the incident electron beam should be parallel to the basal planes of a particular crystallite under study. This was achieved by orienting the crystallite in such a way that in the diffraction mode a systematic row of closely spaced diffraction spots of the type (00.*l*) was visible over its whole length. Bright-field (BF) lattice fringe images were obtained by admitting the transmitted beam and the (00.2) and (00.4) diffracted beams of the *W* compound through the aperture. Dark-field (DF) lattice fringe images were obtained using beam deflection and selecting five adjacent reflections of the (00.*l*) row. The observed fringes in perfect *W* correspond to the 00.2 planes with a spacing of 16.4 Å. The dark field image of a particular area is roughly the negative of the bright-field image and usually produced the better contrast.

For the *W* compound (00.*l**) reflections with *l** = odd are forbidden, but may be excited due to double diffraction of, e.g., (10.*l**) reflections. Since these double-diffraction spots may give rise to double-width fringe images (d = 32.8 Å) which can make the interpretation of fringe images difficult, their occurrence on the (00.*l*) row was avoided by appropriate tilting of the specimen.

Results

All specimens contained *W* as the major phase, as evidenced by the electron diffraction patterns and the spacing of lattice fringe images. In sample III the *X* phase was occasionally found, in coexistence with and oriented parallel to the *W* phase inside the same grains. The M_4S, M_6S, and *M* phases were not detected, presumably due to the fact that their compositions deviate too much from that of *W*.

The *W* crystallites frequently exhibited extended defects, running parallel to the basal plane throughout a whole grain. It will be shown that a local deviation of composition is associated with these defects due to the insertion or the absence of an *M* block or of one or more S^0 blocks. We call these defects compositional faults. When these defects are ordered in some fashion, one may speak of a compound, although these were found mostly on a very local scale.

Another type of extended defect was observed, with which no local deviation of the composition is associated. One may call them polytypic or sequential faults (*12*). These defects were found to terminate inside a grain.

Defect Analysis

When one has a regular stacking of blocks containing a defect of deviating block size, the defect is imaged either as two light fringes or as two dark fringes at a distance differing from the spacing of the perfect fringe system. Thus to identify a defect in a given lattice fringe image one has to decide which "image code" to take. It was observed that the image code reverses sign when going from BF to DF lattice imaging, and also gradually when passing a thickness contour. In the DF images of the present investigation the image code was such that the size of a defect corresponds with the distance between two dark fringes which is either smaller or larger than the fringe spacing of perfect *W*. This was decided by comparing the image widths of the defects for the two image

codes with the theoretical sizes of M, MS_2, or MS_3 blocks. In no case were defect sizes corresponding to that of single R, S, or T blocks found. From a micrograph showing a large number of defects of the same type, sometimes even occurring in an ordered array, the defect width could be accurately determined by simply averaging. The width of isolated defects was measured from a microddensitometer profile across the defect or by using an eyepiece.

Compositional Faults

The defects which were observed most frequently in sample I could be identified as isolated S^0 blocks, whereas sample III contained predominantly extra M blocks. The isolated S^0 blocks are not imaged separately, but together with an adjacent W block as WS units. In some cases, double sets of S^0 blocks, imaged as WS_2 units or triple sets of S^0 blocks, imaged as WS_3 units were also observed. Figures 2 and 3 are examples where these three defects, indicated by 1, 2, and 3 respectively, and the isolated M blocks occur in the same crystallite of W. The heavy faulting in the grain is also evidenced by streaking of the 00.l diffraction spots (see inset of Fig. 2).

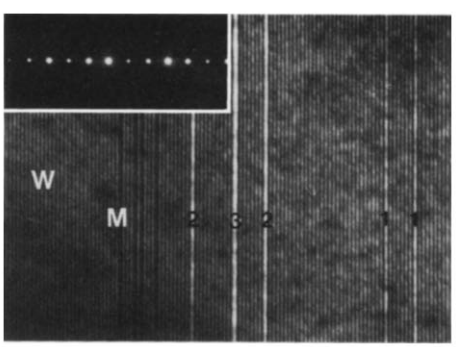

FIG. 2. DF image of W crystallite (fringe distance 16.4 Å) in sample I with extended defects: (1) WS unit of 21.2 Å; (2) WS_2 unit of 26.0 Å; (3) WS_3 unit of 30.8 Å. M indicates four extra M blocks of 11.6 Å. Inset shows 00.l diffraction spots.

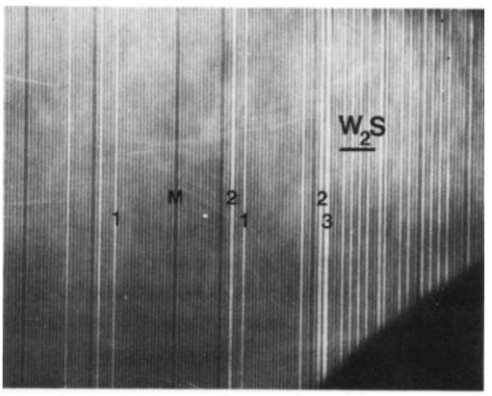

FIG. 3. DF image of W crystallite (sample I) with extended defects and, at the right, an area showing W_2S ordering.

These isolated faults are called compositional faults because a local change of composition is associated with them. Invariably they were found to run through the whole crystallite from grain boundary to grain boundary.

It is noticed that in the WS, WS_2, and WS_3 stripes no fine structure due to insertion of extra S is observed. This may not be so remarkable since the lattice image of perfect W does not show a fine structure of S and M, or even of R blocks either. This is in contrast to the lattice image of pure X, which shows an alternating sequence of M and W fringes. Probably the presence and location of the highly scattering Ba or Sr ions determine which blocks are imaged. Another reason for the absence of S-block fringes in our investigation could be the use of too small an objective aperture, not admitting diffracted rays from the relatively small (4.8 Å) S blocks.

New Phases

In some cases the WS defects or the isolated M blocks were locally found to be present in an ordered array with W blocks. As an example, Fig. 4 (sample I) shows an ordering of WS blocks after each three W blocks, giving rise to a new compound,

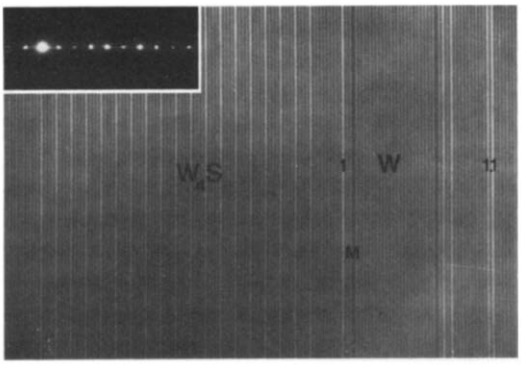

FIG. 4. DF image showing ordering of *WS* units (1) into W_4S. The image also shows two isolated *M* blocks and two adjacent *WS* units (indicated by 1.1).

W_4S or M_4S_5. This phase can be considered as *W* with a missing *M* block every fifth *W* block.

Figure 3 (sample I) shows, at the right, a small region where some *WS* blocks alternate with *W* blocks to form very locally a phase W_2S or M_2S_3. This can be considered as *W* with a missing *M* block every third *W* block.

Figure 5 (sample III) shows a region where *M* blocks have ordered with *W* blocks to give rise to the phase W_3M or M_4S_3. This phase can be regarded as *W* with a missing S^0 block every fourth *W* layer. Here, at two sites, a deviation of the W_3M regularity occurs, with four and two *W* blocks between two *M* blocks.

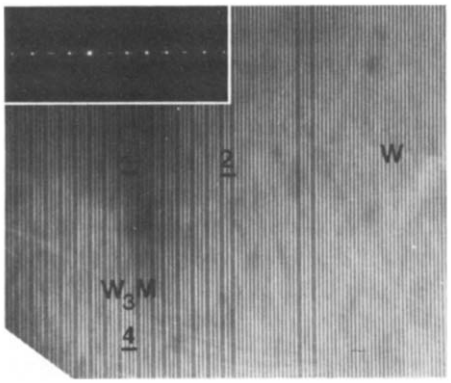

FIG. 5. DF image of *W* (sample III) showing ordering of extra *M* blocks into W_3M. At 2 and 4 two and four *W* blocks, respectively, are observed between two *M* blocks. The image also shows two isolated *M* blocks.

Sequential Faults

A type of fault which was observed frequently, especially in the hot-pressed sample, is shown in Figs. 6a and b, which are bright- and dark-field images, respectively, of the same region in a *W* crystallite of sample II. It is seen that DF image of the defect is the negative of its BF image. Identification of this type of defect presented some difficulties. It is observed in Fig. 6 that these defects terminate inside the crystallite. By viewing along the *W* fringes directly adjacent to the defect, it is seen that they remain straight near the defect edges. The image of the defect in fact consists of two parts, one with a smaller and the other with a larger fringe distance than that of *W*, the sum of which is equal to

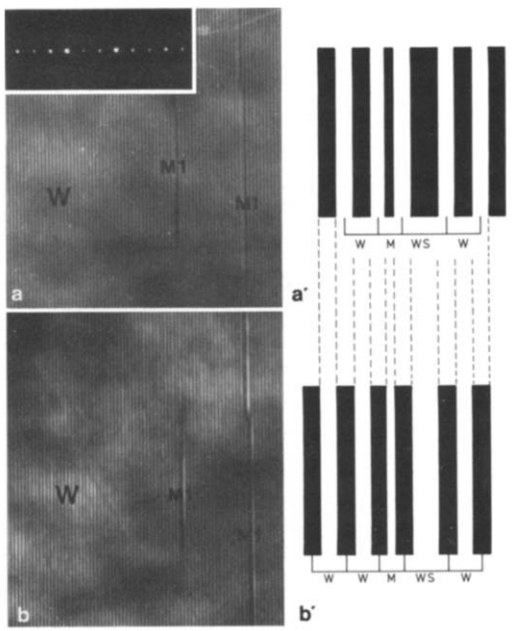

FIG. 6. (a) BF image of *W* crystallite in sample II showing two sequential faults. (a') Interpretation of Fig. 6a. (b) DF image of the same area. (b') Interpretation of Fig. 6b.

two *W* fringes. Thus the total defect has a size equal to that of two *W* blocks. By means of microdensitometer traces across a region containing the defect, and after deciding which image code results in the best correspondence between the defect fringe distances and building blocks with a total width of two *W* blocks, it was concluded that the defects in Fig. 6 consist of an *M* block and a *WS* block next to each other, as indicated in Figs. 6a′ and b′.

In the same crystallite faults of the reverse order, i.e., *WS–M* were also observed.

Three possible sequences of *M* and *S* blocks in a sequential fault can be envisaged:

(a) . . . MSMSMS*MSSM*MSMSMS . . . ,
(b) . . . SMSMSMS*MMSS*MSMSMSM . . . ,
(c) . . . MSMSMS*SSMM*MSMSMS . . . .

In case (a), the fault can be considered to be caused by one inversion in the *M–S* sequence. It cannot be decided here how the defect is imaged, either as *WS–M* or *M–SW*. In view of the *M–S* sequence we tentatively prefer the first possibility.

In case (b), which is the mirror image of case a, the fault is due to one inversion of the *S–M* sequence and will also be imaged as *WS–M* or *M–WS*. Here we prefer the latter possibility. It is likely that the two image faults *WS–M* and *M–WS* which we observed in the same crystal are due to the symmetrical types (a) and (b). In case (c), the fault is more complex, not being due to a single *M–S* inversion. We do not consider it likely that this fault is observed, because it is probably imaged as WS_2–M—M.

From the present observations it cannot be concluded what the precise stacking sequence in the observed sequential faults is. This is only possible by means of a rigorous image computation and comparison with the observed image. It can only be said that these faults are associated *M* and *WS* blocks, the latter having either an *MSS* or an *SSM* stacking sequence.

Discussion

From the present study it appears that small deviations from the ideal ferrous-*W* composition along the *M–S* composition line can be incorporated either as extra S^0 or as extra *M* blocks. The composition deviation may be such that the overall Fe/Ba ratio differs from the ideal value of 9 or that the Fe^{II}/Fe^{III} ratio is not equal to that of the stoichiometric *W* compound. A possible reason for the latter deviation may be that the oxygen partial pressure during heat treatment had not been the equilibrium one corresponding to stoichiometric *W*. Another reason for the composition deviations may be kinetic in origin in that the solid state reaction leading to the *W* compound was not completed. Evidence for the latter cause is the simultaneous presence of both extra S^0 blocks and *M* blocks inside the same grains. Consequently it cannot be decided whether the extra S^0 and *M* blocks are thermodynamically stable defects under certain conditions of temperature, oxygen partial pressure and composition. If this is indeed the case, one may regard *W* with extra S^0 or *M* blocks as being one-dimensional solid solutions of Fe_3O_4 or $BaFe_{12}O_{19}$, respectively, in *W*. In this connection, it is noted that Neumann and Wijn (*10*) and Lotgering and Vromans (*15*), on the grounds of X-ray diffraction analysis and Fe^{II}/Fe^{III}-ratio determinations deduced the existence of nonstoichiometric *W* with Fe^{III} excess, which they wrote as

$BaFe^{II}_{2-x}\square_x Fe^{III}_{16+2x}O_{27}$. In this description the deviation of stoichiometry is realized by extra Fe^{III} ions and Fe^{II} vacancies on the Fe sublattice, similar to the spinel notation of γ-Fe_2O_3. Whether this point defect structure of ferrous W exists, or whether the Fe^{III} excess is incorporated instead as extra M blocks, cannot be decided yet. It may well be that the formation of extra M blocks occurs after a certain point defect saturation concentration (maximum x) is surpassed. On the other hand, it is conceivable that at the same Fe^{II}/Fe^{III} ratio the microstructure of W with extra M blocks and the point defect W structure are both stable, but at different conditions of overall composition, temperature, and oxygen partial pressure.

In very inhomogeneous W grains double S^0_2 and triple S^0_3 blocks have also been observed. It is questionable whether these are stable defects, or whether they are to be considered as small remnants of Fe_3O_4 or initial stages in the epitaxial precipitation of this phase.

When the composition of a crystallite deviates strongly from that of pure W, the extended defects become more concentrated and tend to order into distinct compounds, such as W_4S and W_2S (Fe^{II} surplus) or W_3M (Fe^{III} surplus). These phases are probably stable under certain conditions, because they have been formed by a diffusion reaction. Our attempts, however, to obtain pure W_4S by reaction between M ($SrFe_{12}O_9$) and S (Fe_3O_4) failed, presumably because the reactions were carried out at the wrong conditions. The preparation of WS, starting from the appropriate amounts of M and S, was not successful either.

The frequent observations of the polytypic or sequential faults deserves some consideration. It is hard to imagine that these faults originate from the association of initially separated extra S^0 and M blocks. It is more likely that they have been formed by accidents in the growth of W and thus are real stacking faults. The ending of these faults inside a crystallite may be an indication that the adjacent WS and M blocks annihilate each other to form two perfectly stacked W blocks at the edges of the faults. At these edges there is no good fit of the stacking sequence in the fault with the adjacent perfect W stacking sequence. These regions may be considered as dislocations in which a rapid interdiffusion may lead to the rearrangement of the perfect W lattice, thus shortening the defect. This process could have started at the grain boundaries in an initial stage where the faults extend throughout a whole grain.

Conclusions

Small deviations from the ideal ferrous W composition along the composition line $BaFe_{12}O_{19}$ (M)–Fe_3O_4 (S) are realized by the occurrence of extended defects. These compositional faults are either isolated (extra) M blocks or isolated S blocks. In a few cases isolated double S_2 and triple S_3 blocks have also been observed. At larger composition deviations the M or S blocks tend to order, forming new compounds M_4S_5, M_2S_3, or M_4S_3, depending on the local composition. In stoichiometric W sequential faults may occur, due to the wrong insertion of M or S blocks in the MS sequence. These faults are proposed as being due to growth accidents.

Acknowledgments

The authors would like to thank Mr. D. Veeneman and Dr. F. K. Lotgering for providing samples, Dr. H. B. Haanstra for advice in the TEM work and Dr. M. P. A. Viegers and Ir. F. Kools for useful discussions.

References

1. P. B. Braun, *Philips Res. Rep.* **12,** 491 (1957).
2. J. Smit and H. P. J. Wijn, "Ferrites," Chap. IX, Wiley, New York (1959).
3. J. A. Kohn and D. W. Eckart, *Z. Kristallogr.* **119,** 454 (1964).

4. D. W. ECKART AND J. A. KOH, *Z. Kristallogr.* **125,** 130 (1967).
5. C. F. COOK, JR., *J. Appl. Phys.* **38,** 2488 (1967).
6. J. A. KOHN, D. W. ECKART, AND C. F. COOK, JR., *Mater. Res. Bull.* **2,** 55 (1967).
7. J. A. KOHN, D. W. ECKART, AND C. F. COOK, JR., *Science* **172,** (3983), 519 (1971).
8. H. P. J. WIJN, *Nature* **170,** (433), 707 (1952).
9. H. NEUMANN AND H. P. J. WIJN, *J. Amer. Ceram. Soc.* **51,** 536 (1968).
10. Y. GOTO, M. HIGASHIMOTO, AND K. TAKAHASHI, *Japan. J. Appl. Phys.* **12,** 945 (1973).
11. J. VAN LANDUYT, S. AMELINCKX, J. A. KOHN, AND D. W. ECKART, *Mater. Res. Bull.* **8,** 339 (1973); **8,** 1173 (1973).
12. J. VAN LANDUYT, S. AMELINCKX, J. A. KOHN, AND D. W. ECKART, *J. Solid State Chem.* **9,** 103 (1974).
13. Y. HIROTSU AND H. SATO, *J. Solid State Chem.* **26,** 1 (1978).
14. F. K. LOTGERING, P. H. G. M. VROMANS, AND M. A. H. HUYBERTS, *J. Appl. Phys.* **51,** 5913 (1980).
15. F. K. LOTGERING AND P. H. G. M. VROMANS, *J. Amer. Ceram. Soc.* **60,** 416 (1977).